



## Original article

## Inhibition of monoamine oxidase by selected C6-substituted chromone derivatives

Lesetja J. Legoabe<sup>a</sup>, Anél Petzer<sup>a</sup>, Jacobus P. Petzer<sup>b,\*</sup><sup>a</sup> Unit for Drug Research and Development, School of Pharmacy, North-West University, Private Bag X6001, Potchefstroom 2520, South Africa<sup>b</sup> Pharmaceutical Chemistry, School of Pharmacy, North-West University, Private Bag X6001, Potchefstroom 2520, South Africa

## ARTICLE INFO

## Article history:

Received 15 December 2011

Received in revised form

16 January 2012

Accepted 17 January 2012

Available online 24 January 2012

## Keywords:

Chromone

Monoamine oxidase

Reversible inhibition

Competitive inhibition

Molecular docking

Structure–activity relationship

## ABSTRACT

Chromone has been reported to be a useful scaffold for the design of monoamine oxidase (MAO) inhibitors. In an attempt to discover highly potent MAO inhibitors and to contribute to the known structure–activity relationships (SAR) of MAO inhibition by chromones, in the present study, we have synthesized a series of chromone derivatives substituted at C6 with a variety of alkyloxy substituents, and evaluated the resulting compounds as inhibitors of recombinant human MAO-A and -B. The results document that the C6-substituted chromones are potent reversible MAO-B inhibitors with IC<sub>50</sub> values in the low nM range (2–76 nM). The chromones were also found to bind reversibly to MAO-A, but with lower affinities compared to MAO-B. It may therefore be concluded that C6-substituted chromones are highly potent MAO-B selective inhibitors and promising lead compounds for the development of therapy for neurodegenerative disorders such as Parkinson's disease. The results of this study are discussed with reference to possible binding orientations of a selected C6-substituted chromone in the active site cavities of MAO-A and -B.

© 2012 Elsevier Masson SAS. All rights reserved.

## 1. Introduction

Monoamine oxidase A and B (MAO-A and -B) play essential roles in the catabolism of neurotransmitter amines in central and peripheral tissues [1]. MAO-A selectively catalyzes the oxidation of serotonin while both MAO isoforms utilize dopamine, epinephrine and norepinephrine as substrates [2]. The MAO isozymes not only function to terminate the actions of neurotransmitter amines, but may also protect neurons from stimulation by false neurotransmitters derived from the diet such as benzylamine and  $\beta$ -phenylethylamine [2,3]. These amines are metabolized to a large extent by brain microvessel MAO-B thereby restricting their passage into the brain [4]. The MAO enzymes also serve protective functions as metabolic barriers in the microvessels of the gut wall. Intestinal MAO-A metabolizes tyramine, an indirectly-acting sympathomimetic amine which is present in certain foods. This reduces the amount of tyramine that enters the systemic circulation and prevents the tyramine-induced release of norepinephrine from peripheral neurons [5].

Since MAO-A and -B are involved in the catabolism of dietary and neurotransmitter amines, these enzymes have been targeted

for the therapy of neuropsychiatric and neurodegenerative disorders [2,6,7]. MAO-A inhibitors are used in the treatment of anxiety disorder and depression [2,8] while inhibitors of MAO-B are used in the therapy of Parkinson's disease [9]. In the parkinsonian brain, MAO-B inhibitors block the oxidative metabolism of dopamine in the basal ganglia, thereby conserving the depleted dopamine supply and prolonging its action. Since MAO-B inhibitors also may enhance dopamine levels derived from levodopa, the metabolic precursor of dopamine, MAO-B inhibitors are frequently used as adjunct to levodopa therapy [10,11]. In addition, MAO-B inhibitors may also result in an increase in striatal extracellular dopamine levels by inhibiting the catabolism of  $\beta$ -phenylethylamine, which is both a releaser of dopamine as well as an inhibitor of active dopamine uptake [12]. Although MAO-B is present in higher concentrations than MAO-A in the human basal ganglia [13,14], MAO-A inhibitors have also been shown to enhance dopamine levels in this region. For example, clorgyline, a selective irreversible inhibitor of MAO-A, elevates dopamine levels in the striatum of primates treated with levodopa to a similar degree than the elevation obtained with (*R*)-deprenyl, a selective irreversible inhibitor of MAO-B [11]. In order to conserve dopamine in the basal ganglia, mixed MAO-A/B inhibitors may therefore be more efficacious than selective inhibitors [1].

MAO-B inhibitors are also thought to protect against the neurodegenerative processes implicated in Parkinson's disease by

\* Corresponding author. Tel.: +27 18 2992206; fax: +27 18 2994243.

E-mail address: [jacques.petzer@nwu.ac.za](mailto:jacques.petzer@nwu.ac.za) (J.P. Petzer).

reducing the formation of dopanal and  $H_2O_2$ , metabolic by-products of dopamine oxidation by MAO [15–18]. Dopanal has been implicated in the aggregation of  $\alpha$ -synuclein, a process which is associated with the pathogenesis of Parkinson's disease [19], while  $H_2O_2$  may lead to oxidative damage and promote apoptotic signalling events [20]. Considering that ageing is associated with an increase in the concentration and activity of MAO-B in the central nervous system [13,21,22], inhibition of MAO-B in the aged parkinsonian brain may be of particular relevance. The inhibition of dopamine oxidation would lead to a reduction of harmful dopamine-derived oxidation products and possibly protection against further neuronal damage.

In the search for novel inhibitors of MAO, coumarin (benzopyran-2-one) (**1**) has emerged as a particularly promising scaffold (Fig. 1) [23]. Coumarins are members of the benzopyrone class of compounds which possess diverse pharmacological properties. Substituted coumarins have been shown to act as competitive inhibitors of both MAO-A and -B, with substitution at C7 of the coumarin ring yielding particularly potent MAO-B inhibitors. Another benzopyrone, chromone (benzopyran-4-one) (**2**) has also been shown to be a useful scaffold for the design of MAO inhibitors. For example, a variety of C2- and C3-substituted chromone derivatives have been found to act as potent inhibitors of MAO-B [24,25] and literature reports that a small series of C6- and C7-substituted chromones possesses affinities for both MAO isozymes [23]. The present study investigates the MAO inhibitory properties of a series of chromone derivatives (**3**) substituted at C6 of the benzopyrone ring with a variety of alkoxy substituents. The aim of this study is to discover novel highly potent MAO inhibitors, and to contribute to the known structure–activity relationships (SAR) of MAO inhibition by chromones. Based on the observation that alkoxy substitution of coumarin leads to compounds endowed with high MAO-binding affinities [23], in the present study, alkoxy substituents (benzyloxy, phenylethoxy and phenylpropoxy) were also selected for substitution at C6 of the chromone ring (Table 1). Among these, the benzyloxy side chain has been shown to be particularly suited for enhancing the MAO inhibition potencies of coumarin [23]. We have therefore further explored the MAO inhibition properties of 6-benzyloxychromone (**3a**) by substitution on the benzyloxy phenyl ring with alkyl groups ( $CH_3$ ,  $CN$ ,  $CF_3$ ) and halogens (Cl, Br, F).

## 2. Results

### 2.1. Chemistry

The C6-substituted chromone derivatives (**3a–o**) were efficiently synthesized according to the pathway shown in Scheme 1. 6-Hydroxy-4-chromone (**4**) was reacted with the appropriate alkyl

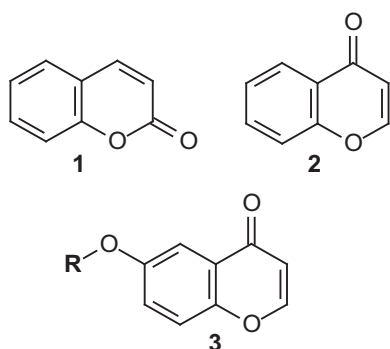


Fig. 1. The structures of coumarin (**1**), chromone (**2**) and the C6-substituted chromone derivatives (**3**) that were investigated in this study.

bromides in the presence of  $K_2CO_3$  to yield the target chromone derivatives in fair yields (21–73%). With the exception of **3b** and **3o**, the products were purified by recrystallization from ethanol. Compounds **3b** and **3o** were purified by column chromatography. In each instance, the structures and purities of the new compounds were verified by  $^1H$  NMR,  $^{13}C$  NMR, mass spectrometry and HPLC analysis as cited in the experimental section.

### 2.2. $IC_{50}$ values for MAO inhibition

The MAO inhibitory properties of the C6-substituted chromone derivatives were evaluated using recombinant human MAO-A and -B as enzyme sources, and kynuramine as substrate [26,27]. Kynuramine is a mixed MAO-A/B substrate and is oxidized by the MAO isozymes to give 4-hydroxyquinoline. 4-Hydroxyquinoline is a fluorescent metabolite which may readily be measured without interference from kynuramine and the test inhibitors **3a–o**, as these species do not fluoresce, or quench the fluorescence of 4-hydroxyquinoline under the conditions used for the enzyme activity measurements. The inhibition potencies of compounds **3a–o** are expressed as  $IC_{50}$  values which were determined in triplicate from sigmoidal dose–response curves as shown by example in Fig. 2.

#### 2.2.1. MAO-B inhibition studies

The MAO-B inhibitory potencies of the C6-substituted chromone derivatives **3a–o** are shown in Table 2. The results show that all of the C6-substituted chromone derivatives are highly potent inhibitors of MAO-B with  $IC_{50}$  values ranging from 0.002 to 0.076  $\mu M$ . The benzyloxy (**3a**), phenylethoxy (**3b**) and phenylpropoxy (**3c**) substituted chromone derivatives exhibit similar  $IC_{50}$  values for the inhibition of MAO-B (0.021–0.057  $\mu M$ ). This indicates that substitution of chromone at C6 with these side chains are suitable for the design of potent MAO-B inhibitors and that increasing the length of the benzyloxy substituent by 1 or 2 carbon units does not enhance MAO-B inhibition potency to a large degree. It is however noteworthy that the phenylethoxy substituted chromone derivative **3b** ( $IC_{50} = 0.021 \mu M$ ) is approximately twofold more potent as an MAO-B inhibitor than the benzyloxy (**3a**) and phenylpropoxy (**3c**) substituted derivatives. Substitution on the benzyloxy phenyl ring of chromone derivative **3a** with halogens leads to a relatively large enhancement of MAO-B inhibition potency. For example, both *meta* and *para* substitution of the benzyloxy ring with chlorine (**3d** and **3e**) and bromine (**3f** and **3g**) enhance the MAO-B inhibition potency of **3a** by approximately 14–26-fold, while *meta* and *para* substitution with fluorine (**3h** and **3i**) enhance the MAO-B inhibition potency of **3a** by four- sixfold. The chlorine (**3d** and **3e**) and bromine (**3f** and **3g**) substituted benzyloxychromone derivatives are the most potent MAO-B inhibitors identified in this study with  $IC_{50}$  values of 0.002–0.0036  $\mu M$ . For comparison, the literature  $IC_{50}$  values for the inhibition of rat MAO-B by C6- and C7-substituted coumarin derivatives are as low as 1.14 nM [23]. Alkyl substitution of the benzyloxy ring is also associated with enhanced MAO-B inhibition potency. The benzyloxychromone derivatives substituted at the *meta* and *para* positions with the methyl group (**3j** and **3k**) also are more potent inhibitors than the corresponding unsubstituted derivative **3a** with  $IC_{50}$  values of 0.019  $\mu M$  and 0.006  $\mu M$ , respectively. While *para* substitution with nitrile (**3m**;  $IC_{50} = 0.022 \mu M$ ) and trifluoromethyl (**3n**;  $IC_{50} = 0.002 \mu M$ ) groups enhances the MAO-B inhibition potency of **3a**, *meta* substitution with a nitrile (**3l**;  $IC_{50} = 0.076 \mu M$ ) is associated with a slight decrease in inhibition potency. Interestingly, bromine substitution of the phenylethoxy substituted chromone derivative **3b** to yield **3o** ( $IC_{50} = 0.027 \mu M$ ), does not enhance the MAO-B inhibition potency of the

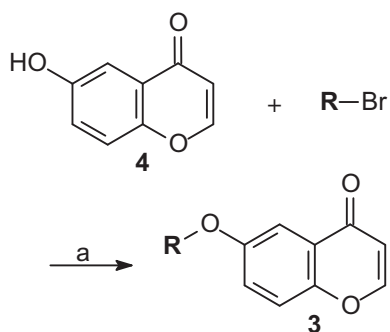
**Table 1**The structures of the C6-substituted chromone derivatives (**3a–o**) that were investigated in this study.

**3**

R	R	R
<b>a</b> 	<b>f</b> 	<b>k</b> 
<b>b</b> 	<b>g</b> 	<b>l</b> 
<b>c</b> 	<b>h</b> 	<b>m</b> 
<b>d</b> 	<b>i</b> 	<b>n</b> 
<b>e</b> 	<b>j</b> 	<b>o</b> 

corresponding unsubstituted phenylethoxy substituted derivative **3b** ( $IC_{50} = 0.021 \mu M$ ). These results demonstrate that substitution with a wide variety of alkyloxy side chains at C6 of chromone leads to structures with potent MAO-B inhibition activity. This relatively

large degree of tolerance for different substituents and substitution patterns make C6-substituted chromone derivatives ideal candidates for the design of MAO-B inhibitors since structural modifications that may lead to better drug properties are less likely to be associated with a loss of activity.



**Scheme 1.** Synthetic pathway to C6-substituted chromone derivatives (**3a–o**). Reagents and conditions: (a)  $K_2CO_3$ , acetone, 24 h.

### 2.2.2. MAO-A inhibition studies

The MAO-A inhibitory potencies of the C6-substituted chromone derivatives **3a–o** are given in Table 2. The results document that the chromone derivatives are also inhibitors of human MAO-A, with most compounds (nine of fifteen) exhibiting  $IC_{50}$  values in the nM range. In spite of their relatively high binding affinities to MAO-A, all of the inhibitors were selective for the MAO-B isozyme as judged by the selectivity index (SI) values. Interestingly, the benzyloxy (**3a**), phenylethoxy (**3b**) and phenylpropoxy (**3c**) substituted chromone derivatives were relatively weak MAO-A inhibitors compared to the other derivatives evaluated in this study, with  $IC_{50}$  values ranging from 1.91 to 3.30  $\mu M$ . Among these three inhibitors, increasing the length of the C6 side chain was associated with

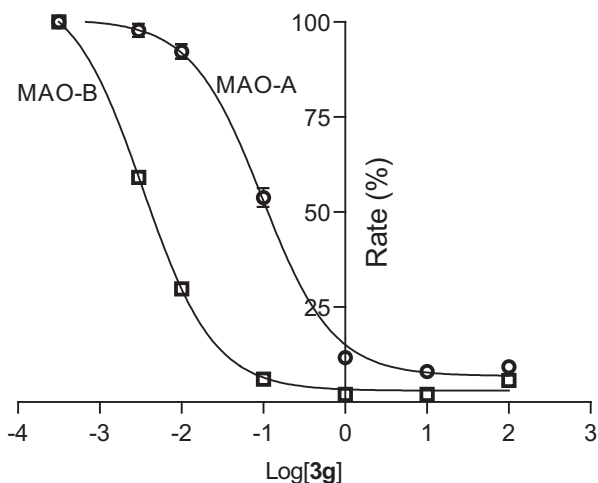
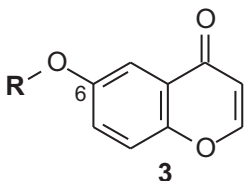


**Fig. 2.** The sigmoidal dose–response curve of the initial catalytic rates of kynuramine oxidation by human MAO-A (circles) and MAO-B (squares) versus the logarithm of the concentration of inhibitor **3g** (expressed in  $\mu\text{M}$ ). The determinations were carried out in triplicate and the values are given as mean  $\pm$  SD.

a modest increase in MAO-A inhibition potency. For example, the benzyloxy (**3a**), phenylethoxy (**3b**) and phenylpropoxy (**3c**) substituted chromone derivatives exhibited  $\text{IC}_{50}$  values towards MAO-A of 3.30  $\mu\text{M}$ , 3.12  $\mu\text{M}$  and 1.19  $\mu\text{M}$ , respectively. Similar to the inhibition studies with MAO-B, substitution on the benzyloxy phenyl ring of **3a** ( $\text{IC}_{50}$  = 3.30  $\mu\text{M}$ ) with chlorine and bromine leads to a relatively large enhancement of MAO-A inhibition potency. For example, both *meta* and *para* substitution of **3a** with chlorine yield compounds **3d** and **3e** with  $\text{IC}_{50}$  values for the inhibition of MAO-A of 0.424  $\mu\text{M}$  and 0.106  $\mu\text{M}$ , respectively, while *meta* and *para*

**Table 2**  
The  $\text{IC}_{50}$  values for the inhibition of recombinant human MAO-A and -B by chromones **3a–o**.



R	$\text{IC}_{50}$ ( $\mu\text{M}$ ) <sup>a</sup>		SI <sup>b</sup>
	MAO-A	MAO-B	
<b>3a</b>	$3.30 \pm 0.176$	$0.053 \pm 0.006$	62
<b>3b</b>	$3.12 \pm 0.213$	$0.021 \pm 0.002$	149
<b>3c</b>	$1.91 \pm 0.083$	$0.057 \pm 0.002$	34
<b>3d</b>	$0.424 \pm 0.041$	$0.0036 \pm 0.001$	118
<b>3e</b>	$0.106 \pm 0.003$	$0.002 \pm 0.0005$	53
<b>3f</b>	$0.386 \pm 0.034$	$0.002 \pm 0.0002$	193
<b>3g</b>	$0.095 \pm 0.010$	$0.0033 \pm 0.001$	29
<b>3h</b>	$1.23 \pm 0.048$	$0.013 \pm 0.001$	95
<b>3i</b>	$0.322 \pm 0.040$	$0.0084 \pm 0.001$	38
<b>3j</b>	$1.13 \pm 0.092$	$0.019 \pm 0.002$	59
<b>3k</b>	$3.49 \pm 0.060$	$0.0060 \pm 0.0006$	582
<b>3l</b>	$0.255 \pm 0.014$	$0.076 \pm 0.003$	3
<b>3m</b>	$0.175 \pm 0.004$	$0.022 \pm 0.009$	8
<b>3n</b>	$0.879 \pm 0.019$	$0.002 \pm 0.0003$	440
<b>3o</b>	$0.480 \pm 0.027$	$0.027 \pm 0.001$	18

<sup>a</sup> All values are expressed as the mean  $\pm$  SD of triplicate determinations.

<sup>b</sup> The selectivity index is the selectivity for the MAO-B isoform and is given as the ratio of  $\text{IC}_{50}$  (MAO-A)/ $\text{IC}_{50}$  (MAO-B).

bromine substitution yield compounds **3f** and **3g** with  $\text{IC}_{50}$  values of 0.368  $\mu\text{M}$  and 0.095  $\mu\text{M}$ , respectively. Compound **3g**, the *para* bromine substituted benzyloxychromone derivative, was found to be the most potent MAO-A inhibitor of this study with an  $\text{IC}_{50}$  value of 0.095  $\mu\text{M}$ . For comparison, the literature  $\text{IC}_{50}$  values for the inhibition of rat MAO-A by C6- and C7-substituted coumarin derivatives are as low as 12.6 nM [23]. Substitution with fluorine at the *para*, and to a lesser degree *meta* positions of the benzyloxy ring, also enhance the MAO-A inhibition potency of **3a**. *Meta* and *para* substitution of the benzyloxy phenyl ring of **3a** with the nitrile group to give compounds **3l** ( $\text{IC}_{50}$  = 0.255  $\mu\text{M}$ ) and **3m** ( $\text{IC}_{50}$  = 0.175  $\mu\text{M}$ ), was also associated with an increase in MAO-A inhibition activity. In contrast, those derivatives substituted at the *meta* and *para* positions with the methyl group (**3j** and **3k**) were relatively weak MAO-A inhibitors among the chromones examined here. In fact, **3k** was found to be the weakest MAO-A inhibitor of the present series with an  $\text{IC}_{50}$  value of 3.49  $\mu\text{M}$ . It is noteworthy that bromine substitution of the phenylethoxy substituted chromone derivative **3b** ( $\text{IC}_{50}$  = 3.12  $\mu\text{M}$ ), to give compound **3o** ( $\text{IC}_{50}$  = 0.480  $\mu\text{M}$ ), leads to an enhancement of the MAO-A inhibition potency. As mentioned above, bromine substitution of the benzyloxy substituted chromone derivative **3a** ( $\text{IC}_{50}$  = 3.30  $\mu\text{M}$ ) yields compound **3g** ( $\text{IC}_{50}$  = 0.095  $\mu\text{M}$ ), also a more potent MAO-A inhibitor than the unsubstituted homologue. Since the bromine substituted benzyloxychromone derivative **3g** is approximately fivefold more potent as an MAO-A inhibitor than the corresponding bromine substituted phenylethoxychromone derivative **3o**, it may be concluded that benzyloxy substitution at C6 of chromone is more beneficial for MAO-A inhibition than phenylethoxy substitution. Another interesting observation is that, among the benzyloxychromone derivatives containing halogen and nitrile substituents on the benzyloxy ring, the *para* substituted homologues were more potent MAO-A inhibitors than the corresponding *meta* substituted chromones. For example, the homologue containing chlorine in the *para* position (**3e**) displayed an  $\text{IC}_{50}$  value towards MAO-A of 0.106  $\mu\text{M}$  while the homologue containing chlorine in the *meta* position (**3d**) displayed an  $\text{IC}_{50}$  value of 0.424  $\mu\text{M}$ . Similarly, the benzyloxychromone derivatives containing bromine (**3g**;  $\text{IC}_{50}$  = 0.095  $\mu\text{M}$ ), fluorine (**3i**;  $\text{IC}_{50}$  = 0.322  $\mu\text{M}$ ) and the nitrile group (**3m**;  $\text{IC}_{50}$  = 0.175  $\mu\text{M}$ ) on the *para* position of the benzyloxy ring were more potent MAO-A inhibitors than the corresponding homologues containing bromine (**3f**;  $\text{IC}_{50}$  = 0.386  $\mu\text{M}$ ), fluorine (**3h**;  $\text{IC}_{50}$  = 1.23  $\mu\text{M}$ ) and the nitrile group (**3l**;  $\text{IC}_{50}$  = 0.255  $\mu\text{M}$ ) on the *meta* position.

### 2.3. Reversibility of MAO inhibition

Based on their interactions with the enzymes, MAO inhibitors may be classified as reversible or irreversible. Irreversible MAO inhibitors, which normally form covalent complexes with the enzymes, have been extensively used as clinical drugs. Irreversible inhibition may however have certain disadvantages [28]. Among these are slow and variable rates of enzyme recovery following withdrawal of the irreversible inhibitor [29]. It has been reported that the turnover rate for the biosynthesis of MAO-B in the human brain may require as much as 40 days [30]. In contrast, following withdrawal of a reversible inhibitor, enzyme activity is recovered when the inhibitor is eliminated from the tissues. In addition, when the reversible inhibition is of a competitive nature, an increase of the substrate concentration will relieve the inhibition. For these reasons the discovery of new MAO inhibitors which act reversibly with the enzymes may be of value.

To determine whether C6-substituted chromone derivatives act as reversible or irreversible inhibitors of MAO-A and -B, the time dependencies of inhibition were examined [31]. For this purpose

compound **3g** was selected as representative inhibitor of this class of compounds. The selection of **3g** was based on the observation that **3g** is a potent inhibitor of both MAO-A and -B among the test compounds. When the enzyme is preincubated in the presence of a reversible inhibitor for various periods of time, the enzyme activity would remain unchanged regardless of the time period for which the inhibitor is incubated with the enzyme. When the enzyme is preincubated in the presence of an irreversible inhibitor, a time-dependent reduction of enzyme activity would be observed. Compound **3g** was preincubated for various time periods (0–60 min) with human MAO-A and -B at concentrations of 0.190  $\mu\text{M}$  and 0.064  $\mu\text{M}$ , respectively. These concentrations of the inhibitor are approximately twofold the measured  $\text{IC}_{50}$  values for the inhibition of MAO-A and -B by **3g**. After addition of the substrate, kynuramine, the residual enzyme activities were measured and bar graphs were constructed. These graphs, presented in Fig. 3, show that preincubation of **3g** with either MAO-A or -B do not lead to a time-dependent reduction in the catalytic activities of these enzymes. These results indicate that **3g** is not a time-dependent inhibitor of human MAO-A and -B over the time period (0–60 min) and at the inhibitor concentrations ( $2 \times \text{IC}_{50}$ ) evaluated. Compound **3g**, and most likely the other chromones examined in this study, are therefore reversible MAO-A and -B inhibitors. Interestingly, a slight increase of catalytic activity as a function of time is observed when **3g** is preincubated with both

MAO-A and -B. While an explanation for this observation is not readily apparent, **3g** may undergo slow hydrolysis in the aqueous buffer (potassium phosphate 100 mM, pH 7.4) used in this study for the enzyme incubations, to yield the corresponding *ortho*-hydroxyphenyl ketone. As a result, the concentration of the active chromone inhibitor may slowly decrease which results in a lesser degree of inhibition and therefore an increase in enzyme catalytic rate. It should be noted that only a relatively small loss of inhibition activity is observed, even after 60 min preincubation of **3g** (Fig. 3). This suggests that only a modest reduction of **3g** concentration occurred in the aqueous incubation medium during the time (20 min) required to carry out the  $\text{IC}_{50}$  determinations, and that the proposed chemical degradation event did not significantly affect the measured  $\text{IC}_{50}$  value.

Based on the observation that **3g** interacts reversibly with MAO-A and -B, the possibility that **3g** acts as a competitive inhibitor of these enzymes was explored. For this purpose, Lineweaver–Burk plots were constructed by measuring the initial catalytic rates of MAO-A and -B in the absence and presence of three different concentrations of **3g**. As shown in Fig. 4, the Lineweaver–Burke plots constructed for the inhibition of MAO-A and -B, respectively, are linear and each set has a common y-intercept. This behaviour is indicative that **3g** is a competitive inhibitor of the MAO isozymes and offers further support for the finding that **3g** is a reversible MAO inhibitor.

#### 2.4. Docking studies

The availability of the X-ray crystal structures of MAO-A and -B greatly aids in the discovery and design of novel inhibitors of these enzymes. Crystallographic and biochemical data show that MAO-A and -B are anchored to the outer mitochondrial membrane via C-terminal transmembrane helices [32,33]. Both enzymes contain flavin adenine dinucleotide (FAD) as cofactor which is covalently bound to the enzymes via a thio ether linkage between the C8 $\alpha$ -position of the FAD and the side chain of a cysteinyl residue (Cys-406 and Cys-397 in MAO-A and -B, respectively) [34,35]. The active site of MAO-A is reported to consist of a single cavity while the active site of MAO-B consists of an entrance cavity which leads to a larger substrate cavity [32,33]. While the active site of MAO-B, in particular the entrance cavity, is mostly hydrophobic, a small hydrophilic region exists in the substrate cavity in front of the *re* face of the FAD isoalloxazine ring. This area is occupied by highly conserved water molecules and is also the site where the amine functional group of a substrate is predicted to bind [35]. In an attempt to identify potential binding modes and interactions of the C6-substituted chromone derivatives with the active sites of MAO-A and -B, compound **3g** was docked into their respective active sites. The selection of compound **3g** as representative inhibitor was based on the observation that it acts as a highly potent inhibitor of both MAO-A and -B among the chromones examined in this study. As enzyme models, the X-ray crystallographic structures of human MAO-A complexed with harmine (PDB entry: 2Z5X) [32] and human MAO-B in complex with 7-(3-chlorobenzoyloxy)-4-formylcoumarin (PDB entry: 2V60) [36] were selected. The MAO-B model containing the 7-(3-chlorobenzoyloxy)-4-formylcoumarin (**5**) (Fig. 5) may be viewed as particularly relevant for the modelling studies since this model would facilitate comparison of the binding mode of the coumarin moiety of **5** with the chromone moiety of **3g**. For the purpose of the docking study, the CDocker module of Discovery Studio 3.1 [37] was employed (see Experimental section). To establish that this protocol is suitable for predicting potential binding modes of reversible inhibitors in the MAO-A and -B active sites, harmine and **5** were redocked into the active sites of MAO-A and -B, respectively. Since the docked binding

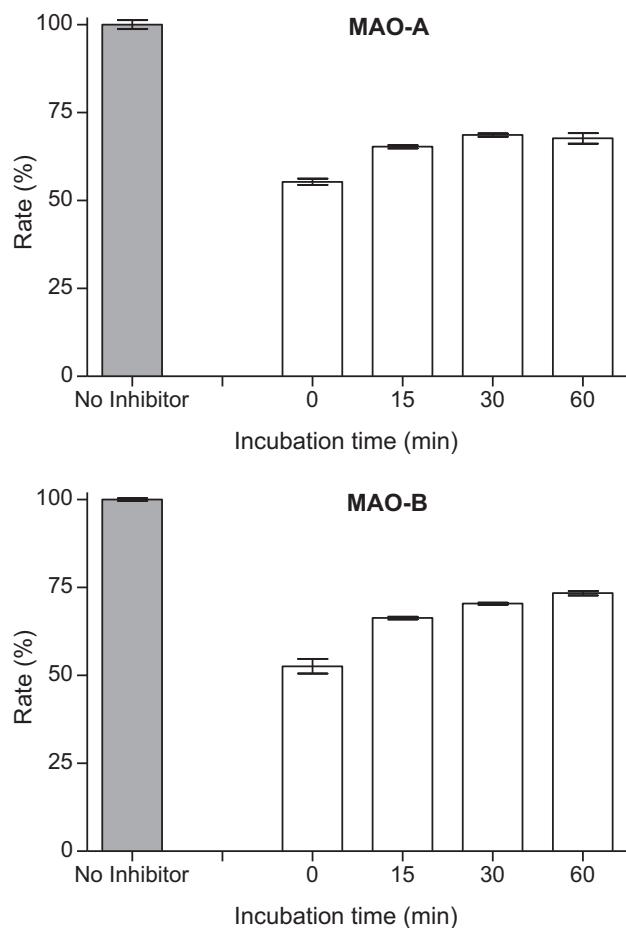


**Fig. 3.** The time-dependant inhibition of human MAO-A (top) and MAO-B (bottom) by **3g**. Compound **3g** was preincubated for various periods of time (0–60 min) with MAO-A and -B at concentrations equal to twofold the  $\text{IC}_{50}$  values for the inhibition of the respective enzymes. After dilution to concentrations of **3g** equal to  $\text{IC}_{50}$ , the residual catalytic rates were recorded.

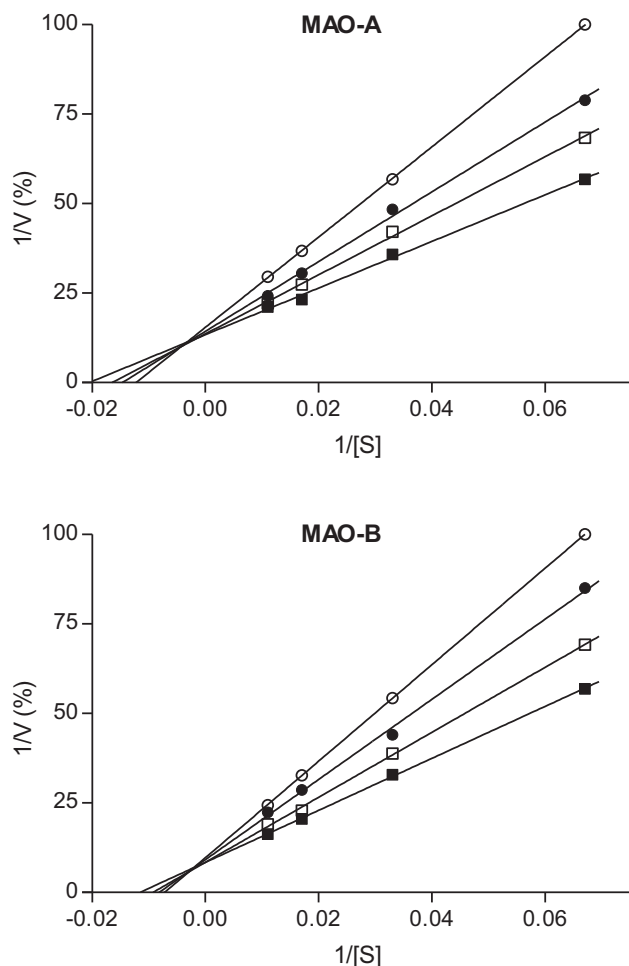


**Fig. 4.** Lineweaver–Burk plots of the rates of oxidation of kynuramine by human MAO-A (top) and MAO-B (bottom) in the absence (filled squares) and presence of various concentrations of **3g**. The inhibitor concentrations selected for the MAO-A studies were: 0.024  $\mu\text{M}$  (open squares), 0.048  $\mu\text{M}$  (filled circles), 0.095  $\mu\text{M}$  (open circles). The inhibitor concentrations selected for the MAO-B studies were: 0.0008  $\mu\text{M}$  (open squares), 0.0016  $\mu\text{M}$  (filled circles), 0.0033  $\mu\text{M}$  (open circles).  $K_i$  values, estimated from a replot of the slopes of the Lineweaver–Burk plots versus inhibitor concentration, are 0.103  $\mu\text{M}$  and 0.004  $\mu\text{M}$  for the inhibition of MAO-A and -B, respectively.

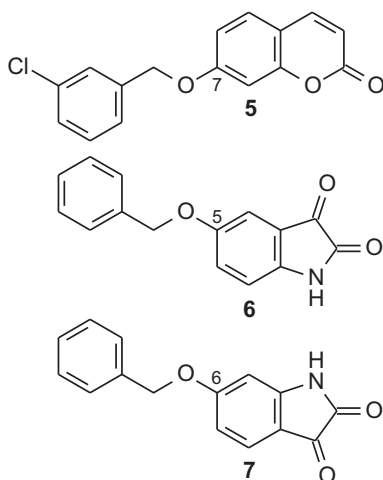


**Fig. 5.** The structures of 7-(3-chlorobenzoyloxy)-4-formylcoumarin (**5**), 5-benzyloxyisatin (**6**) and 6-benzyloxyisatin (**7**).

orientations exhibited relatively small RMSD values of 0.23 Å and 1.62 Å, respectively, from the position of the cocrystallized ligands, this protocol may be considered as suitable for the modelling studies.

The best ranked docking solution of **3g** within the MAO-B active site is illustrated in Fig. 6. The 10 best ranked solutions exhibited highly similar binding orientations with RMSD values of less than 0.01 Å from the position of the best ranked orientation. In the MAO-B active site, the chromone moiety binds within the substrate cavity, in close proximity to the FAD cofactor. The C2 carbon of the chromone moiety is located only 4.1 Å from N5 of the FAD isoalloxazine ring. This position is closer than that of the cocrystallized ligand, compound **5**, which is positioned 5.5 Å from N5 of the isoalloxazine ring. The binding of the **3g** in proximity to the FAD may allow for the formation of a potential  $\pi$ – $\pi$  interaction between the chromone ring and the aromatic ring of Tyr-398. In the substrate cavity, the endocyclic benzopyrone oxygen of **3g** is also within hydrogen bond distance to the phenolic hydrogen of Tyr-398. In the X-ray crystal structure of coumarin **5** in complex with MAO-B, the formyl carbonyl oxygen of **5** is located in the similar region as the benzopyrone oxygen of **3g**, and also interacts via hydrogen bonding with the active site – to a water molecule, as well as the phenolic hydrogen of Tyr-435 [36]. The benzyloxy side chain of **3g** extends to well within the entrance cavity of MAO-B. Since the entrance cavity is lined by hydrophobic amino acid residues, the benzyloxy side chain is most likely stabilized here via hydrophobic interactions [33]. In addition, a potential  $\pi$ – $\sigma$  interaction between the methylene hydrogen of the benzyloxy side chain and the aromatic ring of Tyr-326 may occur. Another potential  $\pi$ – $\sigma$  interaction may also exist between the phenyl ring of **3g** and a side chain hydrogen of Ile-199. Interestingly, in the MAO-B substrate cavity, the chromone ring is rotated by 180° compared to the orientation of the coumarin ring of **5**. A possible explanation for these differing orientations may be that **3g** contains a benzyloxy side chain at C6 of the chromone moiety, while **5** is substituted at C7 of the coumarin ring. This explanation is supported by a previous report that, in the MAO-B substrate cavity, the isatin ring of the reversible MAO inhibitor, 5-benzyloxyisatin (**6**), may also be

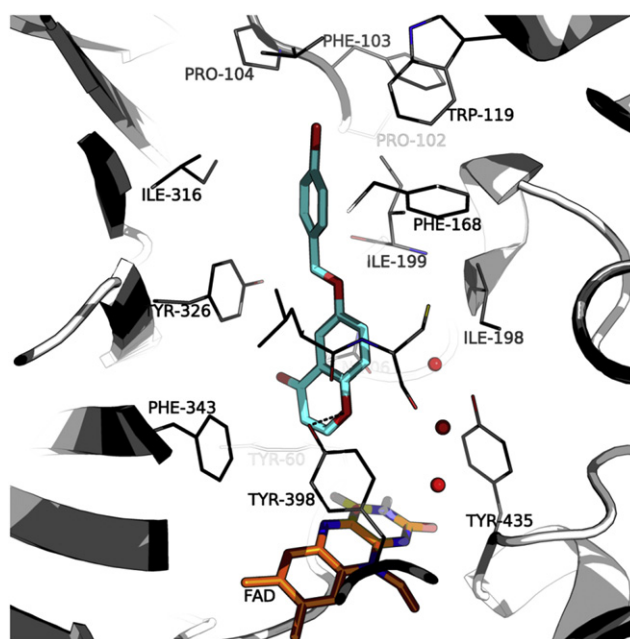


**Fig. 6.** The predicted binding orientation of **3g** within the MAO-B active site.

rotated through  $\sim 180^\circ$  compared to the position of the isatin ring of the 6-benzyloxyisatin isomer (**7**) [31]. These data indicate that the binding orientation of the chromone moiety of **3g** is, to a large degree, guided by the optimal placement of the benzyloxy side chain within the entrance cavity.

The best ranked docking solution of **3g** within the MAO-A active site is given in Fig. 7. Similar to its binding orientation in the MAO-B active site, the chromone moiety of **3g** binds in proximity to the FAD cofactor, only 3.6 Å from N5 of the isoalloxazine ring. This binding mode may allow for the formation of a potential  $\pi$ – $\pi$  interaction between the chromone ring and the aromatic ring of Tyr-444. The benzyloxy substituent of **3g** extends towards the entrance of the active site where the phenyl ring of Phe-208 may undergo a potential  $\pi$ – $\sigma$  interaction with a hydrogen on the benzyloxy ring of **3g**. Compared to the extended orientation of **3g** within the MAO-B active site, in the MAO-A active site **3g** adopt a folded conformation. As discussed in the literature, the folded binding orientations adopted by relatively large inhibitors in the MAO-A active site is to a large degree guided by the aromatic ring of Phe-208 [27]. To avoid structural overlap with Phe-208, larger inhibitors bind in a bent conformation. In the MAO-B active site, the residue that corresponds to Phe-208 in MAO-A, is Ile-199. The small volume of the side chain of Ile-199 allows the side chain of this residue to partially rotate out of the active site, allowing sufficient space for larger inhibitors to bind in an extended conformation [38]. In the MAO-B active site, the benzyloxy ring of **3g** is partly located in space that would have been occupied by the side chain of Ile-199 if it were in the normal “closed” conformation.

### 3. Discussion and conclusion

The present study shows that a series of C6-substituted chromone derivatives (**3a–o**) acts as highly potent reversible MAO-B inhibitors. While all the members of this series were potent MAO-B inhibitors, those containing a benzyloxy substituent at C6 of the chromone moiety, with halogens on the benzyloxy phenyl ring, were the most potent inhibitors with  $IC_{50}$  values equal to, and smaller than 13 nM. As mentioned, the observation that relatively diverse substituents at C6 of the chromone moiety yield structures

with potent MAO-B inhibition activity, suggests that for substitution at C6, a large degree of tolerance for different substituents and substitution patterns exist. This makes C6-substituted chromones suitable lead compounds for the design of MAO-B inhibitors since structural modifications that may improve drug properties are less likely to lead to a loss of activity. Interestingly, the C6-substituted chromones were also reversible inhibitors of MAO-A. In fact, the most potent inhibitor, compound **3g**, exhibited an  $IC_{50}$  value of 0.095  $\mu$ M towards MAO-A. All of the chromones were however selective for the MAO-B isozyme.

Analysis of potential binding orientations of **3g** within the MAO-A and -B active sites shows that, while the inhibitor fits within both active sites, it exhibits differing interactions and orientations within the two enzymes. Most notably, within the MAO-B active site, **3g** interacts via hydrogen bonding with Tyr-398 and exhibits an extended conformation. In the MAO-A active site, **3g** adopts a folded conformation and does not undergo hydrogen bond interactions. These differences may, in part, explain the selectivities of the C6-substituted chromone derivatives for binding to MAO-B. In the MAO-B active site an extended conformation of an inhibitor is considered to be advantageous for binding since this would place part of the inhibitor in the entrance cavity of the enzyme where additional stabilizing interactions may occur [38]. The folded conformation observed in the MAO-A active site may not allow for optimal interaction between the C6 side chain of the chromone derivatives and the enzyme.

In conclusion, C6-substituted chromones are potent reversible MAO-B inhibitors and suitable lead compounds for the development of selective MAO-B inhibitors. Some derivatives also exhibit high binding affinities to MAO-A. Such MAO-A/B mixed inhibitors may be considered particularly promising in the therapy of Parkinson's disease since dopamine is metabolized by both MAO isozymes in the central nervous system. Based on the highly potent MAO inhibitory properties of the chromones examined in this study, further knowledge of their ADME/Tox properties is urgently required.

### 4. Experimental section

#### 4.1. Chemicals and instrumentation

Unless otherwise noted, all reagents and solvents were obtained from Sigma–Aldrich and were used without further purification. Proton ( $^1H$ ) and carbon ( $^{13}C$ ) NMR spectra were recorded in  $CDCl_3$  on a Bruker Avance III 600 spectrometer at frequencies of 600 MHz and 150 MHz, respectively. The chemical shifts are reported in parts per million ( $\delta$ ) downfield from the signal of tetramethylsilane added to the deuterated solvent. Spin multiplicities are given as s (singlet), brs (broad singlet), d (doublet), dd (doublet of doublets), t (triplet), q (quartet), qn (quintet) or m (multiplet). Direct insertion electron impact ionization (EIMS) and high resolution mass spectra (HRMS) were recorded with a DFS high resolution magnetic sector mass spectrometer (Thermo Electron Corporation) in electron ionization (EI) mode. Melting points (mp) were measured with a Buchi M-545 melting point apparatus and are uncorrected. The purities of the synthesized compounds were estimated with HPLC analyses, which were carried out with an Agilent 1100 HPLC system equipped with a quaternary pump and an Agilent 1100 series diode array detector (see Supplementary material). Milli-Q water (Millipore) and HPLC grade acetonitrile (Merck) were used for the chromatography. Fluorescence spectrophotometry was carried out with a Varian Cary Eclipse fluorescence spectrophotometer. Kynuramine·2HBr and insect cell microsomes containing recombinant human MAO-A and -B (5 mg/mL) were obtained from Sigma–Aldrich.

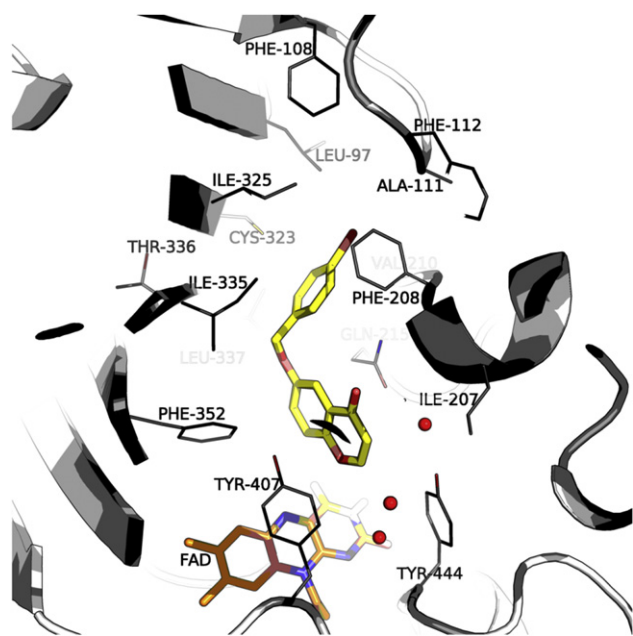


Fig. 7. The predicted binding orientation of **3g** within the MAO-A active site.

#### 4.2. Synthesis of the C6-substituted chromone derivatives (**3a–o**)

To a solution of 6-hydroxy-4-chromone (3 mmol) in 20 mL of acetone, were added anhydrous potassium carbonate (6 mmol) and the appropriate alkyl bromide (6 mmol). The mixture was stirred and heated at reflux for 24 h. The mixture was filtered through a pad of celite and the solvent was removed in vacuo to yield a reddish residue. This crude product was triturated with 50 mL diethyl ether, filtered and dried overnight at 60 °C. For **3b** and **3o**, the residue obtained after removal of the reaction solvent was purified via neutral alumina column chromatography using CH<sub>2</sub>Cl<sub>2</sub>–ethylacetate (4:1) as an eluent. The target chromones were purified by recrystallization from ethanol.

##### 4.2.1. 6-(Benzyloxy)-4H-chromen-4-one (**3a**)

The title compound (dark brown powder) was prepared by reacting 6-hydroxychromone, K<sub>2</sub>CO<sub>3</sub> and benzyl bromide in acetone with yield of 67%: mp 115.9–116.0 °C. <sup>1</sup>H NMR (Bruker Avance III 600 MHz, CDCl<sub>3</sub>) δ 7.82 (d, *J* = 5.9 Hz, 1H), 7.66 (d, *J* = 3.1 Hz, 1H), 7.44 (dd, *J* = 7.9, 1.5 Hz, 2H), 7.41–7.36 (m, 3H), 7.36–7.29 (m, 2H), 6.31 (d, *J* = 5.9 Hz, 1H), 5.12 (s, 2H). <sup>13</sup>C NMR (Bruker Avance III 600 MHz, CDCl<sub>3</sub>) δ 177.46, 156.03, 155.04, 151.45, 136.15, 128.63, 128.20, 127.66, 125.44, 124.33, 119.68, 112.12, 106.01, 70.58. HRMS *m/z*: calcd for C<sub>16</sub>H<sub>12</sub>O<sub>3</sub>, 252.0786, found 252.0793; Purity (HPLC): 99%.

##### 4.2.2. 6-(2-Phenylethoxy)-4H-chromen-4-one (**3b**)

The title compound (dark brown powder) was prepared by reacting 6-hydroxychromone, K<sub>2</sub>CO<sub>3</sub> and 2-phenylethyl bromide in acetone with yield of 73%: mp 118.3–119.4 °C. <sup>1</sup>H NMR (CDCl<sub>3</sub>) δ 7.80 (d, *J* = 5.9 Hz, 1H), 7.54 (d, *J* = 3.1 Hz, 1H), 7.36 (d, *J* = 9.1 Hz, 1H), 7.33–7.26 (m, 4H), 7.23 (m, 2H), 6.29 (d, *J* = 5.9 Hz, 1H), 4.25 (t, *J* = 7.0 Hz, 2H), 3.11 (t, *J* = 6.9 Hz, 2H). <sup>13</sup>C NMR (CDCl<sub>3</sub>) δ 177.41, 156.09, 154.97, 151.28, 137.88, 128.91, 128.47, 126.53, 125.39, 124.06, 119.53, 112.05, 105.60, 69.20, 35.53. HRMS *m/z*: calcd for C<sub>17</sub>H<sub>14</sub>O<sub>3</sub>, 266.0942, found 266.0934; Purity (HPLC): 99%.

##### 4.2.3. 6-(3-Phenylpropoxy)-4H-chromen-4-one (**3c**)

The title compound (off-white powder) was prepared by reacting 6-hydroxychromone, K<sub>2</sub>CO<sub>3</sub> and 3-phenylpropyl bromide in acetone with yield of 51%: mp 177.7–177.8 °C. <sup>1</sup>H NMR (CDCl<sub>3</sub>) δ 7.86 (d, *J* = 5.9 Hz, 1H), 7.56 (d, *J* = 3.0 Hz, 1H), 7.42 (d, *J* = 9.1 Hz, 1H), 7.34–7.27 (m, 3H), 7.27–7.19 (m, 3H), 6.34 (d, *J* = 6.0 Hz, 1H), 4.08 (t, *J* = 6.3 Hz, 2H), 2.85 (t, *J* = 7.5 Hz, 2H), 2.22–2.13 (m, 2H). <sup>13</sup>C NMR (CDCl<sub>3</sub>) δ 177.54, 156.34, 155.00, 151.29, 141.24, 128.45, 125.99, 125.45, 124.10, 119.55, 112.08, 105.56, 67.61, 32.07, 30.64. HRMS *m/z*: calcd for C<sub>18</sub>H<sub>16</sub>O<sub>3</sub>, 280.1099, found 280.1099; Purity (HPLC): 99%.

##### 4.2.4. 6-[(3-Chlorobenzyl)oxy]-4H-chromen-4-one (**3d**)

The title compound (off-white powder) was prepared by reacting 6-hydroxychromone, K<sub>2</sub>CO<sub>3</sub> and 3-chlorobenzyl bromide in acetone with yield of 47%: mp 117.0–117.4 °C. <sup>1</sup>H NMR (CDCl<sub>3</sub>) δ 7.82 (d, *J* = 6.0 Hz, 1H), 7.62 (d, *J* = 3.1 Hz, 1H), 7.46–7.37 (m, 2H), 7.36–7.27 (m, 4H), 6.31 (d, *J* = 5.9 Hz, 1H), 5.09 (s, 2H). <sup>13</sup>C NMR (CDCl<sub>3</sub>) δ 177.35, 155.69, 155.07, 151.55, 138.20, 134.55, 129.89, 128.29, 127.50, 125.48, 125.46, 124.23, 119.82, 112.15, 105.98, 69.64. HRMS *m/z*: calcd for C<sub>16</sub>H<sub>11</sub>ClO<sub>3</sub>, 286.0397, found 286.0395; Purity (HPLC): 99%.

##### 4.2.5. 6-[(4-Chlorobenzyl)oxy]-4H-chromen-4-one (**3e**)

The title compound (off-white powder) was prepared by reacting 6-hydroxychromone, K<sub>2</sub>CO<sub>3</sub> and 4-chlorobenzyl bromide in acetone with yield of 41%: mp 169.5–171.1 °C. <sup>1</sup>H NMR (CDCl<sub>3</sub>) δ 7.82 (d, *J* = 5.9 Hz, 1H), 7.68–7.59 (m, 1H), 7.48–7.26 (m, 6H), 6.35–6.24 (m, 1H), 5.08 (s, 2H). <sup>13</sup>C NMR (CDCl<sub>3</sub>) δ 177.37, 155.75,

155.07, 151.52, 134.66, 134.01, 128.92, 128.81, 125.44, 124.26, 119.78, 112.15, 106.03, 69.75. HRMS *m/z*: calcd for C<sub>16</sub>H<sub>11</sub>ClO<sub>3</sub>, 286.0397, found 286.0395; Purity (HPLC): 98%.

##### 4.2.6. 6-[(3-Bromobenzyl)oxy]-4H-chromen-4-one (**3f**)

The title compound (brown powder) was prepared by reacting 6-hydroxychromone, K<sub>2</sub>CO<sub>3</sub> and 3-bromobenzyl bromide in acetone with yield of 48%: mp 106.7–107.0 °C. <sup>1</sup>H NMR (CDCl<sub>3</sub>) δ 7.74 (d, *J* = 5.9 Hz, 1H), 7.54–7.49 (m, 2H), 7.38–7.29 (m, 2H), 7.29–7.19 (m, 2H), 7.19–7.12 (m, 1H), 6.22 (d, *J* = 6.0 Hz, 1H), 4.99 (s, 2H). <sup>13</sup>C NMR (CDCl<sub>3</sub>) δ 177.36, 155.69, 155.08, 151.56, 138.45, 131.24, 130.42, 130.17, 125.97, 125.45, 124.24, 122.72, 119.83, 112.16, 105.98, 69.58. HRMS *m/z*: calcd for C<sub>16</sub>H<sub>11</sub>BrO<sub>3</sub>, 329.9892, found 329.9889; Purity (HPLC): 99%.

##### 4.2.7. 6-[(4-Bromobenzyl)oxy]-4H-chromen-4-one (**3g**)

The title compound (brown powder) was prepared by reacting 6-hydroxychromone, K<sub>2</sub>CO<sub>3</sub> and 4-bromobenzyl bromide in acetone, with yield of 21%: mp 179.6–180.2 °C. <sup>1</sup>H NMR (CDCl<sub>3</sub>) δ 7.82 (d, *J* = 6.0 Hz, 1H), 7.61 (d, *J* = 3.1 Hz, 1H), 7.54–7.45 (m, 2H), 7.39 (d, *J* = 9.1 Hz, 1H), 7.34–7.26 (m, 3H), 6.30 (d, *J* = 5.9 Hz, 1H), 5.07 (s, 2H). <sup>13</sup>C NMR (CDCl<sub>3</sub>) δ 177.35, 155.72, 155.07, 151.52, 135.17, 131.75, 129.20, 125.44, 124.23, 122.13, 119.78, 112.14, 106.03, 69.76. HRMS *m/z*: calcd for C<sub>16</sub>H<sub>11</sub>BrO<sub>3</sub>, 329.9892, found 329.9885; Purity (HPLC): 99%.

##### 4.2.8. 6-[(3-Fluorobenzyl)oxy]-4H-chromen-4-one (**3h**)

The title compound (white powder) was prepared by reacting 6-hydroxychromone, K<sub>2</sub>CO<sub>3</sub> and 3-fluorobenzyl bromide in acetone, with yield of 53%: mp 91.3–91.4 °C. <sup>1</sup>H NMR (CDCl<sub>3</sub>) δ 7.73 (d, *J* = 6.0 Hz, 1H), 7.53 (t, *J* = 2.2 Hz, 1H), 7.37–7.21 (m, 3H), 7.12–6.99 (m, 2H), 6.92 (t, *J* = 8.6 Hz, 1H), 6.21 (d, *J* = 5.6 Hz, 1H), 5.02 (s, 2H). <sup>13</sup>C NMR (CDCl<sub>3</sub>) δ 177.34, 163.74, 162.11, 155.69, 155.06, 151.53, 138.74, 138.69, 130.19, 130.14, 125.43, 124.22, 122.85, 122.83, 119.79, 115.08, 114.94, 114.35, 114.21, 112.13, 106.00, 69.65. HRMS *m/z*: calcd for C<sub>16</sub>H<sub>11</sub>FO<sub>3</sub>, 270.0692, found 270.0681; Purity (HPLC): 99%.

##### 4.2.9. 6-[(4-Fluorobenzyl)oxy]-4H-chromen-4-one (**3i**)

The title compound (white powder) was prepared by reacting 6-hydroxychromone, K<sub>2</sub>CO<sub>3</sub> and 4-fluorobenzyl bromide in acetone, with yield of 27%: mp 138.1–138.9 °C. <sup>1</sup>H NMR (CDCl<sub>3</sub>) δ 7.83 (d, *J* = 5.9 Hz, 1H), 7.67–7.59 (m, 1H), 7.46–7.37 (m, 3H), 7.30 (dt, *J* = 9.2, 2.2 Hz, 1H), 7.07 (t, *J* = 8.4 Hz, 2H), 6.31 (d, *J* = 6.0 Hz, 1H), 5.08 (s, 2H). <sup>13</sup>C NMR (CDCl<sub>3</sub>) δ 177.41, 163.42, 161.79, 155.84, 155.06, 151.51, 131.95, 131.93, 129.55, 129.50, 125.45, 124.31, 119.76, 115.64, 115.50, 112.16, 105.99, 69.90. HRMS *m/z*: calcd for C<sub>16</sub>H<sub>11</sub>FO<sub>3</sub>, 270.0692, found 270.0694; Purity (HPLC): 99%.

##### 4.2.10. 6-[(3-Methylbenzyl)oxy]-4H-chromen-4-one (**3j**)

The title compound (white powder) was prepared by reacting 6-hydroxychromone, K<sub>2</sub>CO<sub>3</sub> and 3-methylbenzyl bromide in acetone, with yield of 29%: mp 95.2–96.1 °C. <sup>1</sup>H NMR (CDCl<sub>3</sub>) δ 7.82 (d, *J* = 5.9 Hz, 1H), 7.66 (d, *J* = 3.0 Hz, 1H), 7.39 (d, *J* = 9.1 Hz, 1H), 7.35–7.21 (m, 4H), 7.14 (d, *J* = 7.3 Hz, 1H), 6.31 (d, *J* = 5.9 Hz, 1H), 5.08 (s, 2H), 2.36 (s, 3H). <sup>13</sup>C NMR (CDCl<sub>3</sub>) δ 177.43, 156.06, 155.00, 151.40, 138.33, 136.02, 128.96, 128.51, 128.41, 125.42, 124.76, 124.29, 119.63, 112.10, 105.95, 70.64, 21.37. HRMS *m/z*: calcd for C<sub>17</sub>H<sub>14</sub>O<sub>3</sub>, 266.0943, found 266.0937; Purity (HPLC): 99%.

##### 4.2.11. 6-[(4-Methylbenzyl)oxy]-4H-chromen-4-one (**3k**)

The title compound (white powder) was prepared by reacting 6-hydroxychromone, K<sub>2</sub>CO<sub>3</sub> and 4-methylbenzyl bromide in acetone, with yield of 46%: mp 116.5–116.7 °C. <sup>1</sup>H NMR (CDCl<sub>3</sub>) δ 7.82 (d, *J* = 5.9 Hz, 1H), 7.65 (d, *J* = 2.9 Hz, 1H), 7.38 (d, *J* = 9.2 Hz, 1H), 7.35–7.26 (m, 3H), 7.19 (d, *J* = 7.6 Hz, 2H), 6.30 (d, *J* = 5.9 Hz, 1H),

5.08 (s, 2H), 2.34 (s, 3H).  $^{13}\text{C}$  NMR ( $\text{CDCl}_3$ )  $\delta$  177.44, 156.07, 154.99, 151.39, 138.03, 133.10, 129.29, 127.81, 125.42, 124.34, 119.61, 112.10, 105.97, 70.53, 21.18. HRMS  $m/z$ : calcd for  $\text{C}_{17}\text{H}_{14}\text{O}_3$ , 266.0943, found 266.0929; Purity (HPLC): 99%.

#### 4.2.12. 3-[[4-Oxo-4H-chromen-6-yl]oxy]methyl]benzotrile (3l)

The title compound (white powder) was prepared by reacting 6-hydroxychromone,  $\text{K}_2\text{CO}_3$  and 3-cyanobenzyl bromide in acetone, with yield of 29%: mp 155.5–155.8 °C.  $^1\text{H}$  NMR ( $\text{CDCl}_3$ )  $\delta$  7.83 (d,  $J = 5.9$  Hz, 1H), 7.75 (s, 1H), 7.70–7.57 (m, 3H), 7.49 (t,  $J = 7.8$  Hz, 1H), 7.42 (d,  $J = 9.2$  Hz, 1H), 7.33 (dd,  $J = 9.0$ , 2.9 Hz, 1H), 6.31 (d,  $J = 5.7$  Hz, 1H), 5.14 (s, 2H).  $^{13}\text{C}$  NMR ( $\text{CDCl}_3$ )  $\delta$  177.26, 155.38, 155.14, 151.65, 137.81, 131.71, 131.50, 130.68, 129.41, 125.43, 124.17, 119.98, 118.51, 112.80, 112.15, 105.92, 69.10. HRMS  $m/z$ : calcd for  $\text{C}_{17}\text{H}_{11}\text{NO}_3$ , 277.0739, found 277.0733; Purity (HPLC): 99%.

#### 4.2.13. 4-[[4-Oxo-4H-chromen-6-yl]oxy]methyl]benzotrile (3m)

The title compound (white powder) was prepared by reacting 6-hydroxychromone,  $\text{K}_2\text{CO}_3$  and 4-cyanobenzyl bromide in acetone, with yield of 66%: mp 192.6–192.7 °C.  $^1\text{H}$  NMR ( $\text{CDCl}_3$ )  $\delta$  7.82 (d,  $J = 5.6$  Hz, 1H), 7.66 (d,  $J = 7.9$  Hz, 2H), 7.60 (s, 1H), 7.54 (d,  $J = 7.5$  Hz, 2H), 7.41 (d,  $J = 9.0$  Hz, 1H), 7.32 (d,  $J = 9.0$  Hz, 1H), 6.31 (d,  $J = 6.0$  Hz, 1H), 5.18 (s, 2H).  $^{13}\text{C}$  NMR ( $\text{CDCl}_3$ )  $\delta$  177.26, 155.38, 155.15, 151.64, 141.56, 132.41, 127.62, 125.44, 124.12, 119.96, 118.56, 112.16, 111.89, 106.02, 69.33. HRMS  $m/z$ : calcd for  $\text{C}_{17}\text{H}_{11}\text{NO}_3$ , 277.0739, found 277.0732; Purity (HPLC): 95%.

#### 4.2.14. 6-[[4-(Trifluoromethyl)benzyl]oxy]-4H-chromen-4-one (3n)

The title compound (white powder) was prepared by reacting 6-hydroxychromone,  $\text{K}_2\text{CO}_3$  and 4-(trifluoromethyl)benzyl bromide in acetone, with yield of 56%: mp 113.2–113.8 °C.  $^1\text{H}$  NMR ( $\text{CDCl}_3$ )  $\delta$  7.87 (d,  $J = 5.9$  Hz, 1H), 7.68 (d,  $J = 8.3$  Hz, 3H), 7.60 (d,  $J = 7.9$  Hz, 2H), 7.46 (d,  $J = 9.3$  Hz, 1H), 7.37 (dt,  $J = 9.3$ , 2.1 Hz, 1H), 6.35 (d,  $J = 6.0$  Hz, 1H), 5.22 (s, 2H).  $^{13}\text{C}$  NMR ( $\text{CDCl}_3$ )  $\delta$  177.33, 155.61, 155.11, 151.59, 140.20, 130.41, 130.19, 127.50, 125.59 (q), 125.47, 124.89, 124.19, 123.09, 119.88, 112.16, 106.03, 69.60. HRMS  $m/z$ : calcd for  $\text{C}_{17}\text{H}_{11}\text{F}_3\text{O}_3$ , 320.0660, found 320.0659; Purity (HPLC): 99%.

#### 4.2.15. 6-[2-(4-Bromophenyl)ethoxy]-4H-chromen-4-one (3o)

The title compound (white powder) was prepared by reacting 6-hydroxychromone,  $\text{K}_2\text{CO}_3$  and 4-bromophenethyl bromide in acetone with yield of 39%: mp 120.8–120.9 °C.  $^1\text{H}$  NMR ( $\text{CDCl}_3$ )  $\delta$  7.81 (d,  $J = 5.9$  Hz, 1H), 7.52 (d,  $J = 3.1$  Hz, 1H), 7.44–7.33 (m, 3H), 7.26–7.17 (m, 1H), 7.17–7.11 (m, 2H), 6.29 (d,  $J = 6.0$  Hz, 1H), 4.22 (t,  $J = 6.7$  Hz, 2H), 3.05 (t,  $J = 6.7$  Hz, 2H).  $^{13}\text{C}$  NMR ( $\text{CDCl}_3$ )  $\delta$  177.40, 155.94, 155.02, 151.35, 137.01, 131.52, 130.67, 125.40, 124.04, 120.41, 119.62, 112.08, 105.58, 68.74, 34.93. HRMS  $m/z$ : calcd for  $\text{C}_{17}\text{H}_{13}\text{BrO}_3$ , 344.0048, found 344.0033; Purity (HPLC): 96%.

### 4.3. Determination of $\text{IC}_{50}$ values

Microsomes from insect cells containing recombinant human MAO-A and -B served as sources of the respective enzymes.  $\text{IC}_{50}$  values were calculated from sigmoidal dose–response curves constructed by graphing the initial enzyme catalytic rate versus the logarithm of the test inhibitor. For each curve, 6 different inhibitor concentrations spanning at least 3 orders of a magnitude were used. The  $\text{IC}_{50}$  values were determined in triplicate and are expressed as mean  $\pm$  standard deviation (SD). The enzymatic reactions were conducted in potassium phosphate buffer (100 mM, pH 7.4, made isotonic with KCl 20.2 mM) to a final volume of in 500  $\mu\text{L}$  and contained MAO-A or MAO-B (0.0075 mg protein/mL), the substrate, kynuramine, and various concentrations of the test inhibitors (0–100  $\mu\text{M}$ ). Stock solutions of the test inhibitors were prepared in DMSO and added to the reactions to yield

a concentration of 4% DMSO. For the reactions containing MAO-A, the concentration of kynuramine was 45  $\mu\text{M}$  ( $K_m = 16.1$   $\mu\text{M}$ ), while the kynuramine concentration in the reactions containing MAO-B was 30  $\mu\text{M}$  ( $K_m = 22.7$   $\mu\text{M}$ ) [27]. The reactions were incubated for 20 min at 37 °C, terminated by the addition of 400  $\mu\text{L}$  NaOH (2 N) and 1000  $\mu\text{L}$  water, and the concentrations of the MAO generated 4-hydroxyquinoline were subsequently measured by fluorescence spectrophotometry ( $\lambda_{\text{em}} = 310$ ;  $\lambda_{\text{ex}} = 400$  nm) [26]. For this purpose, a linear calibration curve constructed with known amounts of 4-hydroxyquinoline (0.047–1.56  $\mu\text{M}$ ) was employed. The calibration standards were prepared to a volume of 500  $\mu\text{L}$  in potassium phosphate buffer (100 mM, pH 7.4) and contained 4% DMSO. To each standard was also added 400  $\mu\text{L}$  NaOH (2 N) and 1000  $\mu\text{L}$  distilled water. The rate data were fitted to the one site competition model incorporated into the Prism software package (GraphPad).

### 4.4. Time-dependent studies

To determine whether the inhibition of MAO-A and -B by the chromone derivatives is reversible or irreversible, the time-dependence of inhibition of a selected inhibitor, **3g**, was examined. Compound **3g** was allowed to preincubate with recombinant human MAO-A and -B (0.03 mg/mL) for various periods of time (0, 15, 30, 60 min) at 37 °C in potassium phosphate buffer (100 mM, pH 7.4, made isotonic with KCl). For this purpose, the concentration of **3g** was equal to twofold the measured  $\text{IC}_{50}$  value for the inhibition of MAO-A (0.190  $\mu\text{M}$ ) and MAO-B (0.0064  $\mu\text{M}$ ), respectively. The reactions were subsequently diluted twofold by the addition of kynuramine to yield a final enzyme concentration of 0.015 mg/mL and concentrations of the **3g** that are equal to the  $\text{IC}_{50}$  values. The concentrations of kynuramine were 45  $\mu\text{M}$  and 30  $\mu\text{M}$  for MAO-A and -B, respectively, and the final volume of the reactions was 500  $\mu\text{L}$ . The reactions were incubated at 37 °C for a further 15 min and terminated with the addition of 400  $\mu\text{L}$  NaOH (2 N) and 1000  $\mu\text{L}$  distilled water. The rates of the MAO produced 4-hydroxyquinoline were measured and calculated as described above. All measurements were carried out in triplicate and are expressed as mean  $\pm$  SD [31].

### 4.5. Lineweaver–Burk plots

To examine the mode of MAO-A and -B inhibition by the chromone derivatives, a set consisting of four Lineweaver–Burk plots were constructed. For this purpose compound **3g** was selected as representative inhibitor. The concentrations of **3g** that were selected were 0.024–0.095  $\mu\text{M}$  and 0.0008–0.0033  $\mu\text{M}$  for the inhibition studies with MAO-A and -B, respectively. Kynuramine at concentrations of 15–90  $\mu\text{M}$  served as substrate and recombinant human MAO-A and -B were used at a concentration of 0.015 mg/mL. The initial MAO catalytic rates were measured as described above. Linear regression analysis was performed using GraphPad Prism [31].

### 4.6. Molecular modelling studies

Molecular docking and preparation of the enzyme models were carried out in the Windows based Discovery Studio 3.1 modelling software (Accelrys) [37]. The structure of **3g** was drawn within Discovery Studio, hydrogen atoms were added and its geometry was briefly optimized in Discovery Studio using a Dreiding-like forcefield (5000 iterations). The test ligand was further prepared with the Prepare Ligands application of Discovery Studio and atom potential types and partial charges were assigned with the Momany and Rone CHARMM forcefield. The X-ray crystallographic structures of MAO-A

cocrystallized with harmine (PDB code: 2Z5X) [32] and MAO-B cocrystallized with 7-(3-chlorobenzyloxy)-4-formylcoumarin (5) (PDB code: 2V60) [36] were obtained from the Brookhaven Protein Data Bank ([www.rcsb.org/pdb](http://www.rcsb.org/pdb)). The protonation states and pKa values of the ionizable amino acids residues were calculated and hydrogen atoms were added at pH 7.4 to the models. When necessary, the valences of the FAD cofactors (oxidized state) and cocrystallized inhibitors were corrected and the enzyme models were automatically typed with the Momany and Rone CHARMm forcefield. A fixed constraint was applied to the enzyme backbone and the models were energy minimized using the Smart Minimizer algorithm with the maximum steps set to 50,000. For this procedure the implicit generalized Born solvation model with molecular volume was used. The cocrystallized inhibitors and the backbone constraints were subsequently deleted from the models and the binding sites were identified from an analysis of the enzyme cavities. In both the MAO-A and -B protein models, the cocrystallized water molecules were deleted with the exception of 3 active site waters. Since structures of MAO-B have shown that three active site water molecules (HOH 1159, 1166 and 1309; A-chain of 2V60) are conserved, all in the vicinity of the FAD cofactor they were retained for the simulations [36]. In the MAO-A structure, the crystal waters which occupy the analogous positions in the MAO-A active site (HOH 710, 718 and 739; 2Z5X) to those waters in the MAO-B active site cited above were retained. Docking was subsequently carried out with the CDOCKER protocol allowing for the generation of 10 random ligand conformations and a heating target temperature of 700 K in full potential mode. The docked ligands were finally refined using in situ ligand minimization employing the Smart Minimizer algorithm. Unless otherwise specified, all the application modules within Discovery Studio were set to their default values. The illustrations were generated with PyMOL [39].

## Acknowledgements

The NMR spectra were recorded by André Joubert of the SASOL Centre for Chemistry, North-West University while the MS spectra were recorded by Marelize Ferreira of the Mass Spectrometry Service, University of the Witwatersrand. This work was supported by grants from the National Research Foundation and the Medical Research Council, South Africa.

## Appendix. Supplementary material

Supplementary material associated with this article can be found, in the online version, at [doi:10.1016/j.ejmech.2012.01.037](https://doi.org/10.1016/j.ejmech.2012.01.037).

## References

- [1] M.B.H. Youdim, Y.S. Bakhle, Monoamine oxidase: isoforms and inhibitors in Parkinson's disease and depressive illness, *Br. J. Pharmacol.* 147 (2006) S287–S296.
- [2] M.B.H. Youdim, D.E. Edmondson, K.F. Tipton, The therapeutic potential of monoamine oxidase inhibitors, *Nat. Rev. Neurosci.* 7 (2006) 295–309.
- [3] A.A. Boulton, Phenylethylaminergic modulation of catecholaminergic neurotransmission, *Prog. Neuropsychopharmacol. Biol. Psychiatry* 15 (1991) 139–156.
- [4] F. Lasbennes, R. Sercombe, J.J. Seylaz, Monoamine oxidase activity in brain microvessels determined using natural and artificial substrates: relevance to the blood-brain barrier, *Cereb. Blood Flow. Metab.* 3 (1983) 521–528.
- [5] M. Da Prada, G. Zürcher, I. Würthrich, W.E. Haefely, On tyramine, food beverages and the reversible MAO inhibitor moclobemide, *J. Neural Transm.* 26 (1988) 33–56.
- [6] M.B.H. Youdim, M. Weinstock, Therapeutic applications of selective and non-selective inhibitors of monoamine oxidase A and B that do not cause significant tyramine potentiation, *Neurotoxicology* 25 (2004) 243–250.
- [7] P. Riederer, L. Lachenmayer, G. Laux, Clinical applications of MAO-inhibitors, *Curr. Med. Chem.* 11 (2004) 2033–2043.
- [8] S.E. Zisook, Clinical overview of monoamine oxidase inhibitors, *Psychosomatics* 26 (1985) 240–251.
- [9] H.H. Fernandez, J.J. Chen, Monoamine oxidase-B inhibition in the treatment of Parkinson's disease, *Pharmacotherapy* 27 (2007) 1745–1855.
- [10] J.P. Finberg, J. Wang, K. Bankiewicz, J. Harvey-White, I.J. Kopin, D.S. Goldstein, Increased striatal dopamine production from L-DOPA following selective inhibition of monoamine oxidase B by R(+)-N-propargyl-1-aminoindan (rasagiline) in the monkey, *J. Neural Transm.* 52 (1998) 279–285.
- [11] D.A. Di Monte, L.E. DeLanney, I. Irwin, J.E. Royland, P. Chan, M.W. Jacowec, J.W. Langston, Monoamine oxidase-dependent metabolism of dopamine in the striatum and substantia nigra of L-DOPA-treated monkeys, *Brain Res.* 738 (1996) 53–59.
- [12] J.P. Finberg, I. Lamensdorf, T. Armoni, Modification of dopamine release by selective inhibitors of MAO-B, *Neurobiology (Bp)* 8 (2000) 137–142.
- [13] R.N. Kalaria, M.J. Mitchell, S.I. Harik, Monoamine oxidases of the human brain and liver, *Brain* 111 (1988) 1441–1451.
- [14] G.G.S. Collins, M. Sandler, E.D. Williams, M.B.H. Youdim, Multiple forms of human brain monoamine oxidase, *Nature* 225 (1970) 817–820.
- [15] M. Gesi, A. Santinami, R. Ruffoli, G. Conti, F. Fornai, Novel aspects of dopamine oxidative metabolism confounding outcomes take place of certainties, *Pharmacol. Toxicol.* 89 (2001) 217–224.
- [16] F. Fornai, G. Battaglia, M. Gesi, F.S. Giorgi, F. Orzi, F. Nicoletti, Time-course and dose-response study on the effects of chronic L-DOPA administration on striatal dopamine levels and dopamine transporter following MPTP toxicity, *Brain Res.* 887 (2000) 110–117.
- [17] S.A. Marchitti, R.A. Deitrich, V. Vasiliou, Neurotoxicity and metabolism of the catecholamine-derived 3,4-dihydroxyphenylacetaldehyde and 3,4-dihydroxyphenylglycolaldehyde: the role of aldehyde dehydrogenase, *Pharmacol. Rev.* 59 (2007) 125–150.
- [18] I. Lamensdorf, G. Eisenhofer, J. Harvey-White, A. Nechustan, K. Kirk, I.J. Kopin, 3,4-Dihydroxyphenylacetaldehyde potentiates the toxic effects of metabolic stress in PC12 cells, *Brain Res.* 868 (2000) 191–201.
- [19] V.J. Burke, V.B. Kumar, N. Pandey, W.M. Panneton, Q. Gan, M.W. Franko, M. O'Dell, S.W. Li, Y. Pan, H.D. Chung, J.E. Galvin, Aggregation of  $\alpha$ -synuclein by DOPAL, the monoamine oxidase metabolite of dopamine, *Acta Neuropathol.* 115 (2008) 193–203.
- [20] J.K. Mallajosyula, D. Kaur, S.J. Chinta, S. Rajagopalan, A. Rane, D.G. Nicholls, D.A. Di Monte, H. Macarthur, J.K. Andersen, B. MAO, Elevation in mouse brain astrocytes results in Parkinson's pathology, *PLoS One* 3 (2008) e1616.
- [21] A. Nicotra, F. Pierucci, H. Parvez, O. Santori, Monoamine oxidase expression during development and aging, *Neurotoxicology* 25 (2004) 155–165.
- [22] J.S. Fowler, N.D. Volkow, G.J. Wang, J. Logan, N. Pappas, C. Shea, R. MacGregor, Age-related increases in brain monoamine oxidase B in living healthy human subjects, *Neurobiol. Aging* 18 (1997) 431–435.
- [23] C. Gnerre, M. Catto, F. Leonetti, P. Weber, P.-A. Carrupt, C. Altomare, A. Carotti, B. Testa, Inhibition of monoamine oxidases by functionalized coumarin derivatives: biological activities, QSARs, and 3D-QSARs, *J. Med. Chem.* 43 (2000) 4747–4758.
- [24] A. Gaspar, T. Silva, M. Yáñez, D. Viña, F. Orallo, F. Ortuso, E. Uriarte, S. Alcaro, F. Borges, Chromone, a privileged scaffold for the development of monoamine oxidase inhibitors, *J. Med. Chem.* 54 (2011) 5165–5173.
- [25] A. Gaspar, J. Reis, A. Fonseca, N. Millhazes, D. Viña, E. Uriarte, F. Borges, Chromone 3-phenylcarboxamides as potent and selective MAO-B inhibitors, *Bioorg. Med. Chem. Lett.* 21 (2011) 707–709.
- [26] L. Novaroli, M. Reist, E. Favre, A. Carotti, M. Catto, P.A. Carrupt, Human recombinant monoamine oxidase B as reliable and efficient enzyme source for inhibitor screening, *Bioorg. Med. Chem.* 13 (2005) 6212–6217.
- [27] B. Strydom, S.F. Malan, N. Castagnoli Jr., J.J. Bergh, J.P. Petzer, Inhibition of monoamine oxidase by 8-benzylxocaffeine analogues, *Bioorg. Med. Chem.* 18 (2010) 1018–1028.
- [28] L.H.A. Prins, J.P. Petzer, S.F. Malan, Inhibition of monoamine oxidase by indole and benzofuran derivatives, *Eur. J. Med. Chem.* 45 (2010) 4458–4466.
- [29] K.F. Tipton, S. Boyce, J. O'Sullivan, G.P. Davey, J. Healy, Monoamine oxidases: certainties and uncertainties, *Curr. Med. Chem.* 11 (2004) 1965–1982.
- [30] J.S. Fowler, N.D. Volkow, J. Logan, G. Wang, R.R. MacGregor, D. Schlyer, A.P. Wolf, N. Pappas, D. Alexoff, C. Shea, E. Dorflinger, L. Kruchow, K. Yoo, E. Fazzini, C. Patlak, Slow recovery of human brain MAO B after L-deprenyl (selegiline) withdrawal, *Synapse* 18 (1994) 86–93.
- [31] C.I. Manley-King, J.J. Bergh, J.P. Petzer, Inhibition of monoamine oxidase by selected C5- and C6-substituted isatin analogues, *Bioorg. Med. Chem.* 19 (2011) 261–274.
- [32] S.-Y. Son, J. Ma, Y. Kondou, M. Yoshimura, E. Yamashita, T. Tsukihara, Structure of human monoamine oxidase A at 2.2-Å resolution: the control of opening the entry for substrates/inhibitors, *Proc. Natl. Acad. Sci. U.S.A.* 105 (2008) 5739–5744.
- [33] C. Binda, P. Newton-Vinson, F. Hubálek, D.E. Edmondson, A. Mattevi, Structure of human monoamine oxidase B, a drug target for the treatment of neurological disorders, *Nat. Struct. Biol.* 9 (2002) 22–26.
- [34] D.E. Edmondson, A. Mattevi, C. Binda, M. Li, F. Hubálek, Structure and mechanism of monoamine oxidase, *Curr. Med. Chem.* 11 (2004) 1983–1993.
- [35] D.E. Edmondson, C. Binda, J. Wang, A.K. Upadhyay, A. Mattevi, Molecular and mechanistic properties of membrane-bound mitochondrial monoamine oxidase, *Biochemistry* 48 (2009) 4220–4230.
- [36] C. Binda, J. Wang, L. Pisani, C. Caccia, A. Carotti, P. Salvati, D.E. Edmondson, A. Mattevi, Structures of human monoamine oxidase B complexes with selective noncovalent inhibitors: safinamide and coumarin analogs, *J. Med. Chem.* 50 (2007) 5848–5852.

- [37] Accelrys Discovery Studio 1.7, Accelrys Software Inc., San Diego, CA, USA, 2006.<http://www.accelrys.com>.
- [38] F. Hubálek, C. Binda, A. Khalil, M. Li, A. Mattevi, N. Castagnoli, D.E. Edmondson, Demonstration of isoleucine 199 as a structural determinant for the selective inhibition of human monoamine oxidase B by specific reversible inhibitors, *J. Biol. Chem.* 280 (2005) 15761–15766.
- [39] W.L. DeLano, The PyMOL Molecular Graphics System, DeLano Scientific, San Carlos, USA, 2002.